KCNK3 channel is important for the ventilatory response to hypoxia in rats

Céline-Hivda Yegen, Mélanie Lambert, Antoine Beurnier, David Montani, Marc Humbert, Carole Planès, Emilie Boncoeur, Nicolas Voituron, Fabrice Antigny

KCNK3 channel is important for the ventilatory response to hypoxia in rats

Céline-Hivda Yegen[1*], Mélanie Lambert[2,3*], Antoine Beurnier[2,3,4], David Montani[2,3,5], Marc Humbert[2,3,5], Carole Planès[1,6], Emilie Boncoeur[1], Nicolas Voituron[1,7§], Fabrice Antigny[2,3§]

1. Laboratoire Hypoxie & Poumon, UMR INSERM U1272, Université Sorbonne Paris Nord, Bobigny, France.

2. Université Paris-Saclay, Faculté de Médecine, Le Kremlin-Bicêtre, France

3. INSERM UMR_S 999 « Hypertension pulmonaire : Physiopathologie et Innovation Thérapeutique », Hôpital Marie Lannelongue, Le Plessis-Robinson, France.

4. Service de Physiologie et d'explorations fonctionnelles, Hôpital Avicenne, APHP, Hôpitaux de Paris, France

5. Assistance Publique - Hôpitaux de Paris (AP-HP), Service de Pneumologie et Soins Intensifs Respiratoires, Centre de Référence de l'Hypertension Pulmonaire, Hôpital Bicêtre, Le Kremlin-Bicêtre, France.

6. AP-HP, Department of Physiology – Functional Explorations, DMU Thorinno, bi-site Hôpital Bicêtre (Le Kremlin Bicêtre) and Ambroise Paré (Boulogne-Billancourt), France

7. Département STAPS, Université Sorbonne Paris Nord, Bobigny, France.

*These authors contributed equally to this work

§ These authors contributed equally to this work

Correspondence: fabrice.antigny@inserm.fr (F.A.); nicolas.voituron@sorbonne-paris-nord.fr (N.V.); Tel.: +(33)-140-942-299 (F.A.); +(33)- 148-387-632 (N.V).

Abstract: To clarify the contribution of KCNK3/TASK-1 channel chemoreflex in response to hypoxia and hypercapnia, we used a unique *Kcnk3-deficient* rat. We assessed ventilatory variables using plethysmography in *Kcnk3-deficient* and wild-type rats at rest in response to hypoxia (10% O_2) and hypercapnia (4% CO_2). Immunostaining for *C-Fos*, a marker of neuronal activity, was performed to identify the regions of the respiratory neuronal network involved in the observed response.

Under basal conditions, we observed increased minute ventilation in *Kcnk3-deficient* rats, which was associated with increased *c-Fos* positive cells in the ventrolateral region of the medulla oblongata. *Kcnk3-deficient* rats show an increase in ventilatory response to hypoxia without changes in response to hypercapnia. In *Kcnk3-deficient* rats, linked to an increased hypoxia response, we observed a greater increase in c-Fos-positive cells in the first central relay of peripheral chemoreceptors and *Raphe Obscurus*.

This study reports that KCNK3/TASK-1 deficiency in rats induces an inadequate peripheral chemoreflex, alternating respiratory rhythmogenesis, and hypoxic chemoreflex.

Keywords: Hypoxia, Hypercapnia, *c-Fos*, K2P3.1, raphe obscurus

Introduction

In mammals, the regulation of breathing is crucial for maintaining correct blood oxygenation and eliminating carbon dioxide (CO_2). This regulation is controlled by the central and peripheral regions. The regulation of the membrane potential by ion channels contributes to breathing regulation via central and peripheral respiratory chemoreception. Among the ion channels, background K^+ channels play an essential role in maintaining respiratory control (Bayliss et al., 2015; Buckler, 2015). Background K^+ channels are mainly characterised by the two-pore domain potassium (K2P) channel family. K2Ps function as background K^+ conductance channels that help stabilise resting membrane potentials of different cell types (Enyedi and Czirják, 2010). Moreover, non-canonical sensing mechanisms have been observed in K2P channels with rapid gating kinetics (similar to many voltage-gated K^+ channels). These K2P properties suggest they contribute to rapid neuronal action potentials (Schewe et al., 2016).

K2P channels comprise two subunits, each with two pore domains that form a single pore highly selective for K^+ (Enyedi and Czirják, 2010). Among K2P, the potassium channel subfamily K^+ member 3 (KCNK3), also called TWIK-related acid-sensitive K^+ (TASK-1), and KCNK9 or TASK-3 are both described in mice as contributing to the regulation of breathing, using double- or simple-deficient mice for *task-1* or *task-3* (Buehler et al., 2017; Jungbauer et al., 2017). TASK-1 and TASK-3 have several characteristics with the background K^+ current, including minor voltage sensitivity, extracellular pH sensitivity, resistance to classic K^+ channel blockers, and nonsensitivity to cytoplasmic calcium concentrations (Le Ribeuz et al., 2020).

The regulation of peripheral breathing is primarily mediated by the carotid body (Rausch et al., 1991). The predominant channels in rodent carotid body glomus cells are KCNK3/TASK-1 and KCNK9/TASK-3. Electrophysiological and pharmacological approaches have highlighted their presence in the rat carotid body type-1 cells (Buckler et al., 2000; Buckler, 2007). Buckler et al. showed that the TASK channels play a central role in the response of arterial chemoreceptors to hypoxia, acidosis, and hypercapnia (Buckler et al., 2000). Later, using *kcnk3/task-1* or *kcnk9/task-3* knockout mice, the same group demonstrated that both KCNK3/TASK-1 and KCNK9/TASK-3 are inhibited by hypoxia, cyanide, or mitochondrial uncouplers, and that they are coupled to both oxygen and metabolic signalling pathways in these cells (Turner and Buckler, 2013). Moreover, *kcnk3/task-1* knockout mice

showed an almost 50% reduction in hypoxia and CO2 (by 68%)-induced increases in carotid sinus nerve chemoafferent discharge recorded (Trapp et al., 2008). In the carotid body, a hypoxia-induced decrease in TASK-1/TASK-3 function initiates plasma membrane depolarisation, resulting in voltage-gated calcium channel activation and the consecutive activation of neurotransmitters that excite the glossopharyngeal nerve. The afferent glossopharyngeal nerve projects to the pontomedullary respiratory centre through the nucleus of the solitary tract, which allows for adjusting ventilation (López-Barneo et al., 2008). Furthermore, the KCNK3/TASK-1 channel is functionally expressed at multiple levels in brainstem respiratory-related neurones such as airway motoneurons or presumptive chemoreceptor neurones (Bayliss et al., 2001, 2015). However, controversial results have been reported regarding the role of KCNK3/TASK-1 in controlling breathing in response to hypoxia and hypercapnia in mice. *task1*$^{-/-}$ mice have a relatively normal CO_2-chemoreflex, suggesting that these channels are not essential for central respiratory chemosensitivity (Mulkey et al., 2007). In contrast, Trapp and co-workers showed in *task1*$^{-/-}$ and *task1/task3* double knockout mice a 50% and 68% reduction in ventilatory responses to hypoxia and CO_2, respectively, compared to wild-type mice. The ventilatory responses to hypoxia and CO_2 were unchanged in *task3*$^{-/-}$ mice, suggesting that the TASK-3 channel is not required for central respiratory responses while TASK-1 is crucial for the ventilatory regulation in responses to hypoxia and hypercapnia (Trapp et al., 2008). As rats and mice have different adaptation mechanisms in breathing (Arias-Reyes et al., 2021). Moreover, KCNK3/TASK-1 is not functional in mouse pulmonary vasculature contrary to humans and rats (Manoury et al., 2011; Antigny et al., 2016; Kitagawa et al., 2017; Lambert et al., 2019). *task1*$^{-/-}$ mice developed hyperaldosteronism (Heitzmann et al., 2008), whereas aldosterone production is unchanged in *Kcnk3*-deficient rats (Lambert et al., 2019). These examples highlight crucial differences between mice and rats concerning KCNK3/TASK-1, which could exist for ventilatory response to hypoxia or hypercapnia in rats. Moreover, gain-of-function mutations in the *KCNK3* gene were recently identified in patients with sleep apnoea (Sörmann et al., 2022). Patients with sleep apnoea have altered breathing during sleep and develop pulmonary hypertension in 17%–50% of patients with sleep apnoea (Bady et al., 2000; Yan et al., 2021), and KCNK3/TASK-1 dysfunction leads to pulmonary hypertension (Antigny et al., 2016; Lambert et al., 2019).

To clarify the role of KCNK3/TASK-1 in the control of breathing and to determine the role of KCNK3 in the regulation of breathing in rats, we used *Kcnk3-deficient* rats. This study employed a recent and unique *Kcnk3*$^{\Delta 94ex1/\Delta 94ex1}$ rat line with a deficiency in the KCNK3 protein (Lambert et al., 2019, 2021) and characterised the consequence of *Kcnk3* deficiency in the control of breathing in rats.

Methods

Animals and surgical procedures - The animal facility was licenced by the French Ministry of Agriculture (agreement N° C92-019-01). This study was approved by the Committee on Ethics of Animal Experiments (CEEA26; CAP Sud). Animal experiments were approved by the French Ministry of Higher Education, Research, and Innovation (N°7757). Animal experiments were performed in accordance with the guidelines from Directive 2010/63/EU on 22 September 2010 of the European Parliament on the protection of animals used for scientific purposes, and complied with the French institution's animal care and handling guidelines.

Kcnk3-deficient rats

Kcnk3-deficient rats were generated using the CRISPR/Cas 9 technique with a specific sgRNA-rKCNK3 and Cas9 mRNA (Remy et al., 2017; Lambert et al., 2019, 2021) targeting the first exon of the *Kcnk3* gene, to induce a shift in the reading frame of exon 1 of the *Kcnk3* gene. We used a strain with 94 bp deleted in the first exon of *Kcnk3* (Δ94ex1), as previously described (Lambert et al., 2019, 2021). In one new-born rat, a deletion of 94 bp (Δ94ex1) was found, which resulted in an out-of-frame shift in the open reading frame, leading to a premature stop codon and generation of a completely different aa (amino acid) sequence. However, premature stop codons can cause mRNA degradation (Chang et al., 2007). The deletion of 94 bp in the mRNA was not associated with the absence of mRNA, indicating the absence of mRNA degradation (Chang et al., 2007). We studied homozygous rats (*Kcnk3*$^{\Delta 94ex1/\Delta 94ex1}$, also called *Kcnk3*-deficient rats) and wild-type (WT) littermates. Only male rats were analysed in this study at three months old.

As we described (Lambert et al., 2019, 2021), a putative translation of the truncated mRNA could produce a truncated 90-aa protein instead of the 411 aa of the wild-type (WT) protein and share only the first 14 aa with the WT protein. Sequencing of the *Kcnk3* mRNA from *Kcnk3*$^{+/+}$ and *Kcnk3*$^{\Delta 94ex1/\Delta 94ex1}$

rats confirmed the deletion of the 94 bp and an aberrant protein sequence with eight potential premature stop codons (Lambert et al., 2019).

The founder animal with the Δ94ex1 deletion was crossed with a WT partner, and the deletion was transmitted to the offspring, as shown by genotypic DNA analysis, demonstrating that the rats were either *Kcnk3*$^{+/+}$, heterozygous *Kcnk3*$^{\Delta 94ex1/+}$, or homozygous *Kcnk3*$^{\Delta 94ex1/\Delta 94ex1}$. In this study, we used only *Kcnk3*$^{+/+}$ and homozygous *Kcnk3*$^{\Delta 94ex1/\Delta 94ex1}$.

***In vivo* measurement of ventilatory variables -** Ventilatory variables were measured non-invasively in unanaesthetised and unrestrained animals by adapting the technique developed by Drorbaugh and Fenn (Drorbaugh and Fenn, 1955) and modified by Bartlett and Tenney (Bartlett and Tenney, 1970). Briefly, a whole-body flow barometric plethysmograph was used to obtain breathing variables using a differential pressure transducer (model DP 45-18, Validyne Engineering, Northridge, CA, USA) placed between a recording chamber and a reference chamber of the same volume. The pressure signal was sent to a demodulator (model CD15, Validyne Engineering, Northridge, CA), and the breathing variables were recorded using a Spike 2 data analysis system (CED, Cambridge, UK). Rats were placed in the recording chamber ventilated with air at room temperature (21–22°C). Thus, whole-body plethysmography provided a measurement of respiratory frequency (f_R in cycle per min, c/min), mean total time of one breath (Ttot, in seconds), tidal volume (V_T in µl), and minute ventilation (Ve in ml/min). Tidal volume and minute ventilation were normalised by the weight (V_T, µl/g and Ve, ml/g/min). The irregularity score (IS) reflects the variability in the duration of respiratory cycles (Voituron et al., 2009). The delta of Ve was obtained by calculating the difference between the values obtained under normoxia, hypoxia, and hypercapnia at different times for each animal. The Ti/Ttot and V_T/Ti ratios were also determined to indicate breathing time and an index of inspiratory drive (Milic-Emili and Grunstein, 1976).

To evaluate the hypoxic ventilatory response (HVR) and hypercapnic ventilatory response (HcVR), air was replaced with a hypoxic (10% O_2) or hypercapnic (4% CO_2) gas mixture for 10 min. Briefly, measurements were performed under normoxia (21% O_2) for 30 min, followed by hypoxia for 10 min (measures performed at 1’30, 2’30, 5, and 10 min), followed by a 30 min recovery period under normoxia, then hypercapnia for 10 min (measures performed at 1’30, 2’30, 5, and 10 min), followed

again by a recovery period under normoxia (10 min) as described (Voituron et al., 2011). To analyse the response to hypoxia and hypercapnia, the ventilatory parameters were compared with the period of normoxia immediately preceding them. In this way, as the respiratory parameters are expressed as a function of the previous period of normoxia, the hypothetical influence of hypoxia was subtracted.

Analysis of *c-Fos* expression - The rib cage was opened after anaesthetising the rats with an intraperitoneal mixture of ketamine (100 mg/kg) and xylazine (10 mg/kg). Thus, rats were placed in a box ventilated with air (Normoxic condition) or hypoxic gas (O_2 10%-balanced N_2) mixture for 2 hr. Transcardiac perfusion of 0.1M phosphate-buffered saline (PBS) was performed for 10 min at a flow rate of 5ml/min. The animals were then fixed by transcardial perfusion of 4% paraformaldehyde for 15 min. The whole brain of each animal was kept in 4% paraformaldehyde (PFA) for 48 h to optimise post-fixation. The 4% PFA was replaced by a 30% sucrose solution prepared in 0.1M PBS at 4°C. Sections of 40µm thickness were made in the cryostat and then preserved in a cryoprotector based on sucrose and 0.2M PBS to be stored at -20°C. Immunostaining was performed on one of every two sections, and the *c-Fos* protein was detected using standard procedures for Fos-Like Immunohistochemistry on free-floating sections (Perrin-Terrin et al., 2016). Endogenous peroxidases were neutralized with H_2O_2 3%. Sections were then placed in 0.1M PBS supplemented with 0,3% Triton X-100 and 1% bovine serum albumin (BSA). Sections were then incubated for 48h at 4°C with a mouse monoclonal primary antibody directed against the *c-Fos* protein (sc-166940, Santa Cruz Biotechnology Inc., Santa Cruz, CA, USA) diluted 1/2000 in 0.1M PBS supplemented with 0,3% Triton X-100 and 0,5% BSA. Sections were then incubated at room temperature for 2h with a biotinylated horse anti-mouse IgG (BA 2000, Vector Laboratories) diluted 1/1000 in 0.1M PBS supplemented with 0,3% Triton X-100 and 0,5% BSA and for 1h with Avidin-Biotin-Peroxidase complex (VECTASTAIN, Elit PK-100 standard, ZE0622). Peroxidase activity was detected with 0.015% 3,34-diaminobenzidine tetrahydrochloride, 0.04% nickel ammonium sulfate, and 0.006% H_2O_2 in 0.05M Tris buffer (pH 7,6). The reaction was stopped by rinsing with PBS once a brown colouration was visible. Sections were washed, mounted on silane-treated slides, air-dried, dehydrated with absolute alcohol, cleared with xylene, and covered with coverslips.

Control sections were treated in parallel without primary or secondary antibodies. No labelling was observed under these conditions.

Sections were examined under a light microscope (Zeiss Axioskop, Germany), and the region of interest was photographed using a digital camera (Q-Imaging Retiga-200R CDD). *c-Fos* positive cells were quantified at high magnification (x200) using standard landmarks of the medullary respiratory structures (Paxinos: mouse brain in stereotaxic coordinates: compact). Thus, the *c-Fos* positive cells were numbered in the three sub-divisions of the nucleus of the solitary tract: commissural (cNTS), medial (mNTS), and ventrolateral (vlNTS); in the medullary *raphes* nuclei (*raphe obscurus*, ROb; *raphe pallidus*, RPa, and *raphe magnus*, RMg); the caudal and rostral part of the ventrolateral reticular nucleus of the medulla (cVLM and rVLM); and the retrotrapezoid nucleus/parafacial respiratory group (RTN/pFRG) (Joubert et al., 2016; Perrin-Terrin et al., 2016; Jeton et al., 2022; Paxinos: The mouse brain in stereotaxic coordinates: compact).

We previously demonstrated that some neurones do not express c-Fos (Perrin-Terrin et al., 2016). However, this method helps determine the activation of neural pathways, such as respiratory rhythm adaptation, during chemical challenges (Dragunow and Faull, 1989; Perrin-Terrin et al., 2016). As c-Fos staining could also be present in glial cells, we called these cells C-Fos + cells in the present study.

Statistical analysis

All statistical tests were performed using the GraphPad Prism software (GraphPad, version 9.0 for Windows). All values are reported as mean ± standard error of the mean. All data were verified for normal distribution using the Shapiro–Wilk normality test. Differences between groups were analysed using an unpaired t-test for experiments with more than six samples. When the conditions of the parametric tests were not met, we used the Mann-Whitney test. Differences between two or more groups were assessed using a two-way ANOVA. Differences were considered statistically significant at $p < 0.05$.

Results

Breathing at rest

We used whole-body plethysmography to record breathing patterns of freely moving WT and *Kcnk3*$^{\Delta 94ex1/\Delta 94ex1}$ rats under room air. At rest, minute ventilation was significantly increased in *Kcnk3*$^{\Delta 94ex1/\Delta 94ex1}$ rats due to increased V_T (Table 1). Neither respiratory frequency nor variability of the cycle duration expressed by the irregularity score (IS), which reflects the variability in the duration of respiratory cycles, was significantly different between WT and *Kcnk3*$^{\Delta 94ex1/\Delta 94ex1}$ rats (Table 1). The Ti/Ttot ratio (indication of breathing time) was unchanged in *Kcnk3*$^{\Delta 94ex1/\Delta 94ex1}$ rats as compared to that in WT rats, while the V_T/Ti ratio (index of inspiratory drive) was augmented (Table 1).

Consequences of *Kcnk3* deficiency in rats on chemosensitivity to O_2 and CO_2

As described in the Materials and Methods section, in our experimental protocol, we successively exposed the same animal to normoxia and hypoxia, and after the recovery time, to hypercapnia and then normoxia. Before comparing the effects of hypercapnia exposure, we compared the plethysmography values 30 min after hypoxia exposure during the recovery period. As detailed in Table 2, we found similar differences between WT and *Kcnk3*$^{\Delta 94ex1/\Delta 94ex1}$ rats, as indicated by the increased VT, Ve, and Vt/Ti ratio (Table 2).

Concerning the response to hypercapnia, we found that, in WT and *Kcnk3*$^{\Delta 94ex1/\Delta 94ex1}$ rats, hypercapnia significantly increased V_T and f_R without any differences between both groups (Figure 1). Therefore, the increase in Ve in response to CO_2 was similar between WT and *Kcnk3*$^{\Delta 94ex1/\Delta 94ex1}$ rats (Figure 1).

Regarding the ventilatory response to hypoxia, the behaviour of the WT and *Kcnk3*$^{\Delta 94ex1/\Delta 94ex1}$ rats differed. Indeed, in WT rats, we observed a characteristic biphasic response with an increase in Ve (peaking 1 min after the onset of hypoxic exposure), followed by a relative decline (roll-off, Figure 2). This response was due to the biphasic evolution of V_T without a change in f_R. However, in *Kcnk3*$^{\Delta 94ex1/\Delta 94ex1}$ rats, the V_T remained elevated throughout the exposure to hypoxia (Figure 2), leading to a sustained response to hypoxia with an absent or delayed roll-off.

Anatomical substrate responsible for the observed ventilatory response to hypoxia

We sought to identify the ponto-bulbar structures of the respiratory network involved in the observed differences between the mutants and WT rats. Therefore, we performed immunohistochemical detection

of the *c-Fos* protein (black arrow) (Table 3, Figure 3), which could be considered a marker of cellular activity.

Under normoxic conditions, basal *c-Fos* expression was observed in the studied structures (Table 3, Figure 3). Although there was no difference in most structures, we observed an increase of the *c-Fos* positive cells in baseline conditions between WT and *Kcnk3*$^{\Delta 94ex1/\Delta 94ex1}$ rats in the levels of rVLM, cVLM, and *RPa* (Table 3, Figure 3).

In WT rats, hypoxic exposure led to an increase in *c-Fos* expression in cNTS, rVLM, cVLM, *RPa*, and *ROb*, while in *Kcnk3*$^{\Delta 94ex1/\Delta 94ex1}$ rats, hypoxia led to an increase in the number of *c-Fos* positive cells in c and mNTS, as well as in cVLM and *ROb* (Table 3, Figure 3).

Discussion

In this study, we report several essential findings related to the effects of *Kcnk3* deficiency on breathing control. I) Under basal conditions, Ve increases in *Kcnk3*$^{\Delta 94ex1/\Delta 94ex1}$ rats. II) *Kcnk3*$^{\Delta 94ex1/\Delta 94ex1}$ rats developed a potentiated ventilatory response to hypoxia, while the ventilatory response to hypercapnia was unaltered. III) The increased response to hypoxia in *Kcnk3*$^{\Delta 94ex1/\Delta 94ex1}$ rats is associated with a higher number of *c-Fos* positive cells in cNTS, cVLM, and *ROb*.

Role of KCNK3/TASK-1 in breathing control

In a mouse model, the ventilation at rest was similar between WT and *task1*$^{-/-}$ mice (Trapp et al., 2008). In *task1*$^{-/-}$ mice, only modified respiration was observed in male mice (Jungbauer et al., 2017). In *task3*$^{-/-}$ mice, however, discrete changes in respiration were observed in both sexes. Double *task1/task3* knockout (KO) mice exhibit increased basal ventilation caused by an enlarged tidal volume and peak expiratory and inspiratory flow (Buehler et al., 2017). This phenotype was similar to that of *task1*$^{-/-}$ mice (Jungbauer et al., 2017).

In contrast, we found that *Kcnk3*$^{\Delta 94ex1/\Delta 94ex1}$ rats had a higher Ve than WT rats. We only observe a difference in V_T but not in terms of f_R, which would indicate that this increase in Ve was due to a change in the gain of the motor output. This is supported by the increased V_T/Ti ratio, which suggests a strengthening of ventilatory control. In parallel, we observed a difference in *c-Fos* expression in the cVLM. The VLM is a neuronal column ventral to the *ambiguus* nucleus that extends from the pyramidal decussation to the caudal edge of the facial nucleus (Voituron et al., 2006; Huckstepp et al., 2015; Baum

et al., 2018). The ventrolateral medulla contains the ventral respiratory group (VRG) (Bianchi 1971). An increase in phrenic activity amplitude was correlated with an increase in caudal VRG inspiratory neuron activity (Morris et al., 1996), suggesting that strengthening of the ventilatory drive could be linked to the increase in activity observed in the cVLM.

In contrast, we observed an increase in c-Fos activity in the rVLM in the control condition. Catecholaminergic neurons (C1) in the rVLM modulate sympathetic outflow. Indeed, rVLM contains sympatho-excitatory neurones (Guyenet, 2006), which could be responsible for the increased heart rate and right ventricular systolic pressure recently observed in *Kcnk3*$^{\Delta 94ex1/\Delta 94ex1}$ rats (Lambert et al., 2019).

Normal central chemoreflex

The KCNK3/TASK-1 channel and other K2P channels participate in central CO_2/pH chemoreception because of their localisation in various chemosensitive central regions, including the ventrolateral medulla, medullary dorsal, caudal raphe, pontine locus coeruleus, and ventral respiratory group, and because they are sensitive to the external pH and oxygen (Bayliss et al., 2001, 2015; Washburn et al., 2003). In a rat model using the non-selective KCNK3/TASK-1 blocker anandamide, Li Q and colleagues suggested that the KCNK3/TASK-1 channel may act as a chemosensor for central respiration, contributing to pH-sensitive respiratory effects (Li et al., 2020).

However, the role of KCNK3/TASK-1 in the respiratory response to hypercapnia remains controversial. The KCNK3/TASK-1 channel is not involved in central CO_2 chemosensing. Moreover, *task1*$^{-/-}$, *task3*$^{-/-}$ or double *task1/task3* knockout mice have a relatively normal CO_2-chemoreflex, suggesting that these channels are not essential for central respiratory chemosensitivity (Mulkey et al., 2007). Mulkey et al. showed that the pH sensitivity of 5HT raphe neurones was abolished in TASK channel-null mice, indicating that 5HT raphe neurones are not involved in CO2 the chemoreflex (Mulkey et al., 2007). In contrast, Trapp et al. measured altered ventilation in *task1*$^{-/-}$ and *task1/task3* double knockout mice (Trapp et al., 2008). Similarly, to the work of Mulkey et al., we found that exposure to hypercapnia led to a profound increase in ventilation in all animal groups. Furthermore, ventilatory response to hypercapnia was preserved in *Kcnk3*$^{\Delta 94ex1/\Delta 94ex1}$ rats. Similar to that in mice, we demonstrated that KCNK3/TASK-1 was no important in the response to hypercapnia in rats.

However, our results in rats differed from those obtained in *task1*$^{-/-}$ mice, which displayed a blunted respiratory response to hypoxia (Trapp et al., 2008). These differences could be explained by the fact that rats and mice have different adaptation mechanisms (Arias-Reyes et al., 2021), without any doubt regarding our experimental methodology as we and others have already used similar experimental procedures (Voituron et al., 2011; Lucking et al., 2018). In contrast to humans and rats, KCNK3/TASK-1 channels are not functional in mouse pulmonary vasculature (Manoury et al., 2011; Antigny et al., 2016; Kitagawa et al., 2017; Lambert et al., 2019). Moreover, *task1*$^{-/-}$ mice are characterised by hyperaldosteronism (Heitzmann et al., 2008), whereas aldosterone production remains unchanged in *Kcnk3*-deficient rats (Lambert et al., 2019), confirming the crucial differences related to KCNK3/TASK-1 in mice and rats. Moreover, sensitivity to CO_2 differs among rat strains, highlighting the fact that physiological mechanisms, including CO_2 sensitivity, are genetically regulated (Hodges et al., 2002).

Impaired peripheral chemoreflex in *Kcnk3*-deficient rats

In our WT rats, hypoxia induced the classic biphasic ventilatory response, characterised by an increase in ventilation up to a hyperventilation peak, followed by a relative "roll-off" ventilatory depression, where ventilation decreases from the hyperventilation peak but remains above pre-hypoxic values (Maxová and Vízek, 2001). In *Kcnk3*$^{\Delta 94ex1/\Delta 94ex1}$ rats, the first hyperventilation was similar to WT rats. However, roll-off was not observed. Similarly, Trapp et al. demonstrated that after 3 min under hypoxia, the hypoxia-induced increase in ventilation in mice was reduced in *task1*$^{-/-}$ mice (Trapp et al., 2008). We found that WT rats had increased cNTS while *Kcnk3*-deficiency increase cNTS and mNTS. The cNTS and mNTS are significant projection sites from peripheral chemoreceptors (Torrealba and Claps, 1988; Finley and Katz, 1992), suggesting that in addition to carotid bodies, the cNTS and mNTS contribute to breathing regulation in *Kcnk3*-deficient rats. Indeed, carotid body function is compromised in *task1*$^{-/-}$ *mice* (Trapp et al., 2008). In addition, Buckler et al. demonstrated that KCNK3/TASK1 channels may be involved in regulating peripheral chemoreceptor breathing via hypoxic inhibition of KCNK3/TASK-1 channels in carotid body glomus cells (Buckler, 2007, 2015).

As previously mentioned, KCNK3/TASK-1 is expressed in some brainstem respiratory neurones (Bayliss et al., 2001, 2015). In *Kcnk3*$^{\Delta 94ex1/\Delta 94ex1}$ rats (Sprague Dawley strain), we found a more marked increase of *c-Fos* expression in the level of the NTS. At the same time, in this rat strain, orexin neurones

sense extracellular pH changes via TASK channels and participate in ventilatory regulation via projections on the NTS (Wang et al., 2021). Further experiments in *Kcnk3*$^{\Delta 94ex1/\Delta 94ex1}$ rats are needed to understand the consequence of Kcnk3 deficiency entirely.

In WT rats, we observed an increase in the number of *c-Fos* positive cells in *RPa* and *ROb*, as previously observed in response to tissue hypoxia (Bodineau and Larnicol, 2001). In *Kcnk3*$^{\Delta 94ex1/\Delta 94ex1}$ rats, *ROb* was more activated under hypoxic conditions than in WT rats. The *RPa* and *ROb* contain neurones that project to phrenic motoneurons (Loewy and McKellar, 1981; Holtman et al., 1990; Sasek et al., 1990) and structures that generate and modulate the CCR, such as preBötC (Ptak et al., 2009). Therefore, we cannot exclude the possibility that this activation of *ROb* could be implicated in the observed ventilatory response in *Kcnk3*$^{\Delta 94ex1/\Delta 94ex1}$ rats.

Possible consequences of inadequate hypoxic chemoreflex

The fact that the KCNK3/TASK-1 channel contributes to breathing regulation could also have consequences in the development of sleep apnoea, a disorder that affects more than 1 billion people (Benjafield et al., 2019). Interestingly and linked to our present study, Sörmann and colleagues recently identified nine de novo gain-of-function mutations in *KCNK3* that lead to global developmental delay, hypotonia, a range of structural malformations, and sleep apnea (Sörmann et al., 2022). Until this discovery, and due to its expression in the hypoglossal motor nucleus, the link between KCNK3/TASK-1 and sleep apnoea had already been hypothesised (Gurges et al., 2021) but not demonstrated. Furthermore, patients with sleep apnoea experience abnormal, interrupted breathing during sleep, and 17–50% of patients with sleep apnoea develop pulmonary hypertension (Bady et al., 2000; Yan et al., 2021). Although the link between pulmonary hypertension and sleep apnoea remains controversial, nocturnal oxygen drops damage nitric oxide synthesis and cause vascular remodelling, possibly leading to pulmonary hypertension (Dempsey et al., 2010). Moreover, heterozygous loss-of-function mutations in *KCNK3* have been identified in patients with pulmonary arterial hypertension (Ma et al., 2013; Higasa et al., 2017; Olschewski et al., 2017; Le Ribeuz et al., 2020), and we found that *Kcnk3*-deficient rats were predisposed to the development of pulmonary hypertension. Indeed *Kcnk3*$^{\Delta 94ex1/\Delta 94ex1}$ rats developed more severe pulmonary hypertension than WT rats after chronic hypoxia exposure (3 weeks at 10% of O_2) (Lambert et al., 2019). Here we found that in *Kcnk3*$^{\Delta 94ex1/\Delta 94ex1}$ rats, unlike in WT-rats, an

absence of the roll-off respiratory response to hypoxia exposure indicates that *Kcnk3* deficiency impaired response to hypoxia which could contribute to increased susceptibility to the development of lung diseases, including pulmonary hypertension (Lambert et al., 2019, 2021) and possibly sleep apnoea. The increased response to hypoxia in *Kcnk3*-deficient rats could predispose animals to the activation of hypoxia-inducible factor 1 (HIF-1α). HIF-1α is a crucial factor of pulmonary vascular remodelling occurring in PAH (Ryan and Archer, 2015; Lei et al., 2016), and we found an overactivation in HIF-1α in the lung from *Kcnk3*-deficient rats compared to that in WT, which predispose *Kcnk3*-deficient rats to severe PH under chronic-hypoxia exposure (Lambert et al., 2019).

In patients with PAH, a more pronounced increase in minute ventilation than in healthy subjects has been reported during acute hypoxia. This phenomenon is also observed during exercise-induced hypoxia in patients with PAH, which could ameliorate with ventilation-perfusion ratio abnormalities induced by pulmonary vascular disease (Groth et al., 2018). However, further experiments are required to clarify this point.

Conclusions

Using unique *Kcnk3*$^{\Delta 94ex1/\Delta 94ex1}$ rats, we reported that the KCNK3/TASK-1 deficiency alters the effectiveness of structures involved in respiratory rhythmogenesis and the hypoxic chemoreflex arc, probably independently of carotid body structures. These alterations could have profound consequence for patients lacking functional KCNK3/TASK-1, including sleep apnoea and pulmonary hypertension. Nevertheless, further studies are needed to fully elucidate the contribution of KCNK3/TASK-1 to breathing control and sleep apnoea.

Limitations

All commercially available anti-KCNK3 antibodies tested were unusable because when tested in *kcnk3*-knockout mice or in our *Kcnk3*-deficient rats, they were either nonreactive or yielded the same signal as that in WT mice or WT rats (Schmidt et al., 2015; Murtaza et al., 2017; Lambert et al., 2019). This prevented any measurement of KCNK3 protein expression in *Kcnk3*-deficient rats (Lambert et al., 2019). Thus, we could not confirm the localisation of the KCNK3 protein in *Kcnk3*-deficient rats.

Moreover, we found that the ventilatory responses to WT and *Kcnk3*-deficient rats 30 min after hypoxia protocol differ between basal normoxia conditions. To avoid misinterpretation regarding the role of KCNK3/TASK-1 channel in the ventilatory response to hypercapnia, further experiments should be done in different animals to ensure that KCNK3/TASK-1 is not involved in the hypercapnia response.

Authors' contributions: Conception and design: C-H. Y, M.L, N.V, and F.A.; Conducted the experiments and/or performed the data analysis. Y, M. L., N. V., and F.A. All authors drafted and provided important intellectual content for the manuscript. All authors reviewed and approved the final version of the manuscript.

Acknowledgments

This study benefited from the facilities and expertise of TEFOR—Investissement d'avenir—ANR-II-INSBS-0014. We thank Dr. Ignacio Anegon, Laurent Tesson, and Séverine Ménoret from Transgenic Rats and Immunophenomics Core Facility (TRIP), platform TRIP–(Immunology–Nantes) for generating *Kcnk3*$^{\Delta 94ex1/\Delta 94ex1}$ rats. We wish to thank the staff of the ANIMEX platform for providing care to the rat lines.

Conflict of interest

Humbert and Montani had relationships with drug companies, including Actelion, Bayer, GSK, Novartis, and Pfizer. In addition to being investigators in trials involving these companies, other relationships include consultancy services and scientific advisory board membership. The authors have no conflicts of interest to declare.

Sources of Funding

F. Antigny receives funding from the Fondation du Souffle et Fonds de Dotation Recherche en Santé Respiratoire from the Fondation Lefoulon-Delalande and the Fondation Legs Poix. The authors received funding from the National Funding Agency for Research (ANR-18-CE14-0023). NV received funding

from the foundation legs of the Poix, BQR, and IFRB programs of the university Sorbonne Paris Nord. *Kcnk3*-deficient rats were generated with financial support from Fondation maladies rares in the framework of small-animal models, and the rare disease program generated *Kcnk3*-deficient rats. M. Lambert was supported by the Therapeutic Innovation Doctoral School (ED569).

Data availability: The authors declare that all supporting data are available for this study.

Supplementary material: No Supplementary Material.

References

Antigny, F., Hautefort, A., Meloche, J., Belacel-Ouari, M., Manoury, B., Rucker-Martin, C., et al. (2016). Potassium Channel Subfamily K Member 3 (KCNK3) Contributes to the Development of Pulmonary Arterial Hypertension. *Circulation* 133, 1371–1385. doi: 10.1161/CIRCULATIONAHA.115.020951.

Arias-Reyes, C., Soliz, J., and Joseph, V. (2021). Mice and Rats Display Different Ventilatory, Hematological, and Metabolic Features of Acclimatization to Hypoxia. *Front. Physiol.* 12, 647822. doi: 10.3389/fphys.2021.647822.

Bady, E., Achkar, A., Pascal, S., Orvoen-Frija, E., and Laaban, J. P. (2000). Pulmonary arterial hypertension in patients with sleep apnoea syndrome. *Thorax* 55, 934–939. doi: 10.1136/thorax.55.11.934.

Bartlett, D., and Tenney, S. M. (1970). Control of breathing in experimental anemia. *Respir. Physiol.* 10, 384–395. doi: 10.1016/0034-5687(70)90056-3.

Baum, D. M., Saussereau, M., Jeton, F., Planes, C., Voituron, N., Cardot, P., et al. (2018). Effect of Gender on Chronic Intermittent Hypoxic Fosb Expression in Cardiorespiratory-Related Brain Structures in Mice. *Front. Physiol.* 9, 788. doi: 10.3389/fphys.2018.00788.

Bayliss, D. A., Barhanin, J., Gestreau, C., and Guyenet, P. G. (2015). The role of pH-sensitive TASK channels in central respiratory chemoreception. *Pflugers Arch.* 467, 917–929. doi: 10.1007/s00424-014-1633-9.

Bayliss, D. A., Talley, E. M., Sirois, J. E., and Lei, Q. (2001). TASK-1 is a highly modulated pH-sensitive "leak" K(+) channel expressed in brainstem respiratory neurons. *Respir. Physiol.* 129, 159–174. doi: 10.1016/s0034-5687(01)00288-2.

Benjafield, A. V., Ayas, N. T., Eastwood, P. R., Heinzer, R., Ip, M. S. M., Morrell, M. J., et al. (2019). Estimation of the global prevalence and burden of obstructive sleep apnoea: a literature-based analysis. *Lancet Respir. Med.* 7, 687–698. doi: 10.1016/S2213-2600(19)30198-5.

Bodineau, L., and Larnicol, N. (2001). Brainstem and hypothalamic areas activated by tissue hypoxia: Fos-like immunoreactivity induced by carbon monoxide inhalation in the rat. *Neuroscience* 108, 643–653. doi: 10.1016/s0306-4522(01)00442-0.

Buckler, K. J. (2007). TASK-like potassium channels and oxygen sensing in the carotid body. *Respir. Physiol. Neurobiol.* 157, 55–64. doi: 10.1016/j.resp.2007.02.013.

Buckler, K. J. (2015). TASK channels in arterial chemoreceptors and their role in oxygen and acid sensing. *Pflugers Arch.* 467, 1013–1025. doi: 10.1007/s00424-015-1689-1.

Buckler, K. J., Williams, B. A., and Honore, E. (2000). An oxygen-, acid- and anaesthetic-sensitive TASK-like background potassium channel in rat arterial chemoreceptor cells. *J. Physiol.* 525 Pt 1, 135–142. doi: 10.1111/j.1469-7793.2000.00135.x.

Buehler, P. K., Bleiler, D., Tegtmeier, I., Heitzmann, D., Both, C., Georgieff, M., et al. (2017). Abnormal respiration under hyperoxia in TASK-1/3 potassium channel double knockout mice. *Respir. Physiol. Neurobiol.* 244, 17–25. doi: 10.1016/j.resp.2017.06.009.

Chang, Y.-F., Imam, J. S., and Wilkinson, M. F. (2007). The nonsense-mediated decay RNA surveillance pathway. *Annu. Rev. Biochem.* 76, 51–74. doi: 10.1146/annurev.biochem.76.050106.093909.

Dempsey, J. A., Veasey, S. C., Morgan, B. J., and O'Donnell, C. P. (2010). Pathophysiology of sleep apnea. *Physiol. Rev.* 90, 47–112. doi: 10.1152/physrev.00043.2008.

Dragunow, M., and Faull, R. (1989). The use of c-fos as a metabolic marker in neuronal pathway tracing. *J. Neurosci. Methods* 29, 261–265. doi: 10.1016/0165-0270(89)90150-7.

Drorbaugh, J. E., and Fenn, W. O. (1955). A barometric method for measuring ventilation in newborn infants. *Pediatrics* 16, 81–87.

Enyedi, P., and Czirják, G. (2010). Molecular background of leak K+ currents: two-pore domain potassium channels. *Physiol. Rev.* 90, 559–605. doi: 10.1152/physrev.00029.2009.

Finley, J. C. W., and Katz, D. M. (1992). The central organization of carotid body afferent projections to the brainstem of the rat. *Brain Res.* 572, 108–116. doi: 10.1016/0006-8993(92)90458-L.

Groth, A., Saxer, S., Bader, P. R., Lichtblau, M., Furian, M., Schneider, S. R., et al. (2018). Acute hemodynamic changes by breathing hypoxic and hyperoxic gas mixtures in pulmonary arterial and chronic thromboembolic pulmonary hypertension. *Int. J. Cardiol.* 270, 262–267. doi: 10.1016/j.ijcard.2018.05.127.

Gurges, P., Liu, H., and Horner, R. L. (2021). Modulation of TASK-1/3 channels at the hypoglossal motoneuron pool and effects on tongue motor output and responses to excitatory inputs in vivo: implications for strategies for obstructive sleep apnea pharmacotherapy. *Sleep* 44, zsaa144. doi: 10.1093/sleep/zsaa144.

Guyenet, P. G. (2006). The sympathetic control of blood pressure. *Nat. Rev. Neurosci.* 7, 335–346. doi: 10.1038/nrn1902.

Heitzmann, D., Derand, R., Jungbauer, S., Bandulik, S., Sterner, C., Schweda, F., et al. (2008). Invalidation of TASK1 potassium channels disrupts adrenal gland zonation and mineralocorticoid homeostasis. *EMBO J.* 27, 179–187. doi: 10.1038/sj.emboj.7601934.

Higasa, K., Ogawa, A., Terao, C., Shimizu, M., Kosugi, S., Yamada, R., et al. (2017). A burden of rare variants in BMPR2 and KCNK3 contributes to a risk of familial pulmonary arterial hypertension. *BMC Pulm. Med.* 17, 57. doi: 10.1186/s12890-017-0400-z.

Hodges, M. R., Forster, H. V., Papanek, P. E., Dwinell, M. R., and Hogan, G. E. (2002). Ventilatory phenotypes among four strains of adult rats. *J. Appl. Physiol. Bethesda Md 1985* 93, 974–983. doi: 10.1152/japplphysiol.00019.2002.

Holtman, J. R., Vascik, D. S., and Maley, B. E. (1990). Ultrastructural evidence for serotonin-immunoreactive terminals contacting phrenic motoneurons in the cat. *Exp. Neurol.* 109, 269–272. doi: 10.1016/s0014-4886(05)80016-0.

Huckstepp, R. T. R., Cardoza, K. P., Henderson, L. E., and Feldman, J. L. (2015). Role of parafacial nuclei in control of breathing in adult rats. *J. Neurosci. Off. J. Soc. Neurosci.* 35, 1052–1067. doi: 10.1523/JNEUROSCI.2953-14.2015.

Jeton, F., Perrin-Terrin, A.-S., Yegen, C.-H., Marchant, D., Richalet, J.-P., Pichon, A., et al. (2022). In Transgenic Erythropoietin Deficient Mice, an Increase in Respiratory Response to Hypercapnia Parallels Abnormal Distribution of CO2/H+-Activated Cells in the Medulla Oblongata. *Front. Physiol.* 13, 850418. doi: 10.3389/fphys.2022.850418.

Joubert, F., Perrin-Terrin, A.-S., Verkaeren, E., Cardot, P., Fiamma, M.-N., Frugière, A., et al. (2016). Desogestrel enhances ventilation in ondine patients: Animal data involving serotoninergic systems. *Neuropharmacology* 107, 339–350. doi: 10.1016/j.neuropharm.2016.03.041.

Jungbauer, S., Buehler, P. K., Neubauer, J., Haas, C., Heitzmann, D., Tegtmeier, I., et al. (2017). Sex-dependent differences in the in vivo respiratory phenotype of the TASK-1 potassium channel knockout mouse. *Respir. Physiol. Neurobiol.* 245, 13–28. doi: 10.1016/j.resp.2016.11.005.

Kitagawa, M. G., Reynolds, J. O., Wehrens, X. H. T., Bryan, R. M., and Pandit, L. M. (2017). Hemodynamic and Pathologic Characterization of the TASK-1−/− Mouse Does Not Demonstrate Pulmonary Hypertension. *Front. Med.* 4. doi: 10.3389/fmed.2017.00177.

Lambert, M., Capuano, V., Boet, A., Tesson, L., Bertero, T., Nakhleh, M. K., et al. (2019). Characterization of Kcnk3-Mutated Rat, a Novel Model of Pulmonary Hypertension. *Circ. Res.* 125, 678–695. doi: 10.1161/CIRCRESAHA.119.314793.

Lambert, M., Mendes-Ferreira, P., Ghigna, M.-R., LeRibeuz, H., Adão, R., Boet, A., et al. (2021). Kcnk3 dysfunction exaggerates the development of pulmonary hypertension induced by left ventricular pressure overload. *Cardiovasc. Res.* 117, 2474–2488. doi: 10.1093/cvr/cvab016.

Le Ribeuz, H., Capuano, V., Girerd, B., Humbert, M., Montani, D., and Antigny, F. (2020). Implication of Potassium Channels in the Pathophysiology of Pulmonary Arterial Hypertension. *Biomolecules* 10. doi: 10.3390/biom10091261.

Lei, W., He, Y., Shui, X., Li, G., Yan, G., Zhang, Y., et al. (2016). Expression and analyses of the HIF-1 pathway in the lungs of humans with pulmonary arterial hypertension. *Mol. Med. Rep.* 14, 4383–4390. doi: 10.3892/mmr.2016.5752.

Li, Q. Q., Wan, K. X., Xu, M. S., Wang, L. M., Zhang, Y. Y., Wang, C. T., et al. (2020). [The pH-Sensitive Potassium Channel TASK-1 Is a Chemosensor for Central Respiratory Regulation in Rats]. *Mol. Biol. (Mosk.)* 54, 457–468. doi: 10.31857/S0026898420030106.

508 Loewy, A. D., and McKellar, S. (1981). Serotonergic projections from the ventral medulla to the
509 intermediolateral cell column in the rat. *Brain Res.* 211, 146–152. doi: 10.1016/0006-
510 8993(81)90074-3.

511 López-Barneo, J., Ortega-Sáenz, P., Pardal, R., Pascual, A., and Piruat, J. I. (2008). Carotid body oxygen
512 sensing. *Eur. Respir. J.* 32, 1386–1398. doi: 10.1183/09031936.00056408.

513 Lucking, E. F., O'Connor, K. M., Strain, C. R., Fouhy, F., Bastiaanssen, T. F. S., Burns, D. P., et al. (2018).
514 Chronic intermittent hypoxia disrupts cardiorespiratory homeostasis and gut microbiota
515 composition in adult male guinea-pigs. *EBioMedicine* 38, 191–205. doi:
516 10.1016/j.ebiom.2018.11.010.

517 Ma, L., Roman-Campos, D., Austin, E. D., Eyries, M., Sampson, K. S., Soubrier, F., et al. (2013). A novel
518 channelopathy in pulmonary arterial hypertension. *N. Engl. J. Med.* 369, 351–361. doi:
519 10.1056/NEJMoa1211097.

520 Manoury, B., Lamalle, C., Oliveira, R., Reid, J., and Gurney, A. M. (2011). Contractile and
521 electrophysiological properties of pulmonary artery smooth muscle are not altered in TASK-1
522 knockout mice. *J. Physiol.* 589, 3231–3246. doi: 10.1113/jphysiol.2011.206748.

523 Maxová, H., and Vízek, M. (2001). Biphasic ventilatory response to hypoxia in unanesthetized rats.
524 *Physiol. Res.* 50, 91–96.

525 Milic-Emili, J., and Grunstein, M. M. (1976). Drive and timing components of ventilation. *Chest* 70,
526 131–133. doi: 10.1378/chest.70.1_supplement.131.

527 Morris, K. F., Arata, A., Shannon, R., and Lindsey, B. G. (1996). Inspiratory drive and phase duration
528 during carotid chemoreceptor stimulation in the cat: medullary neurone correlations. *J.*
529 *Physiol.* 491 (Pt 1), 241–259. doi: 10.1113/jphysiol.1996.sp021212.

530 Mulkey, D. K., Talley, E. M., Stornetta, R. L., Siegel, A. R., West, G. H., Chen, X., et al. (2007). TASK
531 channels determine pH sensitivity in select respiratory neurons but do not contribute to
532 central respiratory chemosensitivity. *J. Neurosci. Off. J. Soc. Neurosci.* 27, 14049–14058. doi:
533 10.1523/JNEUROSCI.4254-07.2007.

534 Murtaza, G., Mermer, P., Goldenberg, A., Pfeil, U., Paddenberg, R., Weissmann, N., et al. (2017).
535 TASK-1 potassium channel is not critically involved in mediating hypoxic pulmonary
536 vasoconstriction of murine intra-pulmonary arteries. *PloS One* 12, e0174071. doi:
537 10.1371/journal.pone.0174071.

538 Olschewski, A., Veale, E. L., Nagy, B. M., Nagaraj, C., Kwapiszewska, G., Antigny, F., et al. (2017).
539 TASK-1 (KCNK3) channels in the lung: from cell biology to clinical implications. *Eur. Respir. J.*
540 50, 1700754. doi: 10.1183/13993003.00754-2017.

541 Paxinos: The mouse brain in stereotaxic coordinates: compact - Google Scholar (n.d.). Available at:
542 https://scholar.google.com/scholar_lookup?title=The%20Mouse%20Brain%20in%20Stereota
543 xic%20Coordinates&publication_year=2001&author=G.%20Paxinos&author=K.B.%20Franklin
544 [Accessed July 11, 2022].

545 Perrin-Terrin, A.-S., Jeton, F., Pichon, A., Frugière, A., Richalet, J.-P., Bodineau, L., et al. (2016). The c-
546 FOS Protein Immunohistological Detection: A Useful Tool As a Marker of Central Pathways
547 Involved in Specific Physiological Responses In Vivo and Ex Vivo. *J. Vis. Exp. JoVE*. doi:
548 10.3791/53613.

549 Ptak, K., Yamanishi, T., Aungst, J., Milescu, L. S., Zhang, R., Richerson, G. B., et al. (2009). Raphé
550 neurons stimulate respiratory circuit activity by multiple mechanisms via endogenously
551 released serotonin and substance P. *J. Neurosci. Off. J. Soc. Neurosci.* 29, 3720–3737. doi:
552 10.1523/JNEUROSCI.5271-08.2009.

553 Rausch, S. M., Whipp, B. J., Wasserman, K., and Huszczuk, A. (1991). Role of the carotid bodies in the
554 respiratory compensation for the metabolic acidosis of exercise in humans. *J. Physiol.* 444,
555 567–578. doi: 10.1113/jphysiol.1991.sp018894.

556 Remy, S., Chenouard, V., Tesson, L., Usal, C., Ménoret, S., Brusselle, L., et al. (2017). Generation of
557 gene-edited rats by delivery of CRISPR/Cas9 protein and donor DNA into intact zygotes using
558 electroporation. *Sci. Rep.* 7. doi: 10.1038/s41598-017-16328-y.

559 Ryan, J. J., and Archer, S. L. (2015). Emerging concepts in the molecular basis of pulmonary arterial
560 hypertension: part I: metabolic plasticity and mitochondrial dynamics in the pulmonary
561 circulation and right ventricle in pulmonary arterial hypertension. *Circulation* 131, 1691–
562 1702. doi: 10.1161/CIRCULATIONAHA.114.006979.

563 Sasek, C. A., Wessendorf, M. W., and Helke, C. J. (1990). Evidence for co-existence of thyrotropin-
564 releasing hormone, substance P and serotonin in ventral medullary neurons that project to
565 the intermediolateral cell column in the rat. *Neuroscience* 35, 105–119. doi: 10.1016/0306-
566 4522(90)90125-n.

567 Schewe, M., Nematian-Ardestani, E., Sun, H., Musinszki, M., Cordeiro, S., Bucci, G., et al. (2016). A
568 Non-canonical Voltage-Sensing Mechanism Controls Gating in K2P K(+) Channels. *Cell* 164,
569 937–949. doi: 10.1016/j.cell.2016.02.002.

570 Schmidt, C., Wiedmann, F., Voigt, N., Zhou, X.-B., Heijman, J., Lang, S., et al. (2015). Upregulation of
571 K(2P)3.1 K+ Current Causes Action Potential Shortening in Patients With Chronic Atrial
572 Fibrillation. *Circulation* 132, 82–92. doi: 10.1161/CIRCULATIONAHA.114.012657.

573 Sörmann, J., Schewe, M., Proks, P., Jouen-Tachoire, T., Rao, S., Riel, E. B., et al. (2022). Gain-of-
574 function mutations in KCNK3 cause a developmental disorder with sleep apnea. *Nat. Genet.*
575 54, 1534–1543. doi: 10.1038/s41588-022-01185-x.

576 Torrealba, F., and Claps, A. (1988). The vagal connection of the carotid sinus. *Neurosci. Lett.* 93, 186–
577 190. doi: 10.1016/0304-3940(88)90079-1.

578 Trapp, S., Aller, M. I., Wisden, W., and Gourine, A. V. (2008). A role for TASK-1 (KCNK3) channels in
579 the chemosensory control of breathing. *J. Neurosci. Off. J. Soc. Neurosci.* 28, 8844–8850. doi:
580 10.1523/JNEUROSCI.1810-08.2008.

581 Turner, P. J., and Buckler, K. J. (2013). Oxygen and mitochondrial inhibitors modulate both
582 monomeric and heteromeric TASK-1 and TASK-3 channels in mouse carotid body type-1 cells.
583 *J. Physiol.* 591, 5977–5998. doi: 10.1113/jphysiol.2013.262022.

584 Voituron, N., Frugière, A., Champagnat, J., and Bodineau, L. (2006). Hypoxia-sensing properties of the
585 newborn rat ventral medullary surface in vitro. *J. Physiol.* 577, 55–68. doi:
586 10.1113/jphysiol.2006.111765.

587 Voituron, N., Frugière, A., Mc Kay, L. C., Romero-Granados, R., Domínguez-Del-Toro, E., Saadani-
588 Makki, F., et al. (2011). The kreisler mutation leads to the loss of intrinsically hypoxia-

589 activated spots in the region of the retrotrapezoid nucleus/parafacial respiratory group.
590 *Neuroscience* 194, 95–111. doi: 10.1016/j.neuroscience.2011.07.062.

591 Voituron, N., Zanella, S., Menuet, C., Dutschmann, M., and Hilaire, G. (2009). Early breathing defects
592 after moderate hypoxia or hypercapnia in a mouse model of Rett syndrome. *Respir. Physiol.*
593 *Neurobiol.* 168, 109–118. doi: 10.1016/j.resp.2009.05.013.

594 Wang, X., Guan, R., Zhao, X., Chen, J., Zhu, D., Shen, L., et al. (2021). TASK1 and TASK3 in orexin
595 neuron of lateral hypothalamus contribute to respiratory chemoreflex by projecting to
596 nucleus tractus solitarius. *FASEB J.* 35, e21532. doi: 10.1096/fj.202002189R.

597 Washburn, C. P., Bayliss, D. A., and Guyenet, P. G. (2003). Cardiorespiratory neurons of the rat
598 ventrolateral medulla contain TASK-1 and TASK-3 channel mRNA. *Respir. Physiol. Neurobiol.*
599 138, 19–35. doi: 10.1016/s1569-9048(03)00185-x.

600 Yan, L., Zhao, Z., Zhao, Q., Jin, Q., Zhang, Y., Li, X., et al. (2021). The clinical characteristics of patients
601 with pulmonary hypertension combined with obstructive sleep apnoea. *BMC Pulm. Med.* 21,
602 378. doi: 10.1186/s12890-021-01755-5.

603

Table 1: Breathing variables of WT and *Kcnk3*$^{\Delta 94ex1/\Delta 94ex1}$ rats in baseline conditions

	WT n=10	*Kcnk3*$^{\Delta 94ex1/\Delta 94ex1}$ n=9
f_R (c/min)	170 ± 20	159 ± 29
V_T (µl/g)	6.7 ± 1.7	9.6 ±2.2**
V_e (ml/g/min)	1.1 ± 0.3	1.4 ± 0.3*
T_{tot} (sec)	0.36 ± 0.04	0.39 ± 0.06
T_i/T_{tot}	0.62 ± 0.46	0.46 ± 0.13
V_T/T_i	36.8 ± 14.8	60.8 ± 30.9*
IS	7.7 ± 3.9	9.7 ± 5.0

Values are means ± SEM of the respiratory frequency (fR, c/min), tidal volume (V_T; µl/g), minute ventilation (Ve, ml/g/min), mean total time of one breath (T_{tot}, sec), breathing time (Ti/Ttot), index of the inspiratory drive (Vt/Ti) and the, Irregularity score (IS). Data were analysed using an unpaired parametric t-test. * indicates $p<0.05$; ** indicates $p<0.01$.

Table 2: Breathing variables of WT and *Kcnk3*$^{\Delta 94ex1/\Delta 94ex1}$ rats in normoxia condition measured 30 min after hypoxia exposure

	WT *Normoxia 30min after Hypoxia* n=10	*Kcnk3*$^{\Delta 94ex1/\Delta 94ex1}$ *Normoxia 30min after Hypoxia* n=9
f_R (c/min)	129.9 ± 32	119.5 ± 17
V_T (µl/g)	5.38 ± 0.7	8.5 ±0.85*
V_e (ml/g/min)	0.7 ± 0.09	1.1 ± 0.1*
T_{tot} (sec)	0.48 ± 0.09	0.51 ± 0.06
T_i/T_{tot}	0.41 ± 0.02	0.43 ± 0.056
V_T/T_i	29.7 ± 3.8	42.8 ± 5.3*
IS	9.6 ± 2.4	12.9 ± 1.6

Values are means ± SEM of the respiratory frequency (fR, c/min), tidal volume (V_T; µl/g), minute ventilation (Ve, ml/g/min), mean total time of one breath (T_{tot}, sec), breathing time (Ti/Ttot), index of the inspiratory drive (Vt/Ti) and the, Irregularity score (IS). Data were analysed using an unpaired t-test. * indicates $p<0.05$; ** indicates $p<0.01$.

Table 3: Average number of *c-Fos*-positive cells in the medulla oblongata respiratory areas under normoxia and hypoxia in WT and *Kcnk3*$^{\Delta 94ex1/\Delta 94ex1}$ rats.

	WT		*Kcnk3*$^{\Delta 94ex1/\Delta 94ex1}$	
	Normoxia n = 4	Hypoxia n = 9	Normoxia n = 10	Hypoxia n = 8
cNTS	1.8 ± 1.3	5.5 ± 2.4*	3.3 ± 1.2	9.4 ± 3.1*; #
mNTS	2.4 ± 1.6	3.3 ± 1.0	3.9 ± 1.7	6.0 ± 1.9*; #
vlNTS	0.7 ± 0.3	2.3 ± 0.8	1.7 ±1.4	3.5 ± 2.4
cVLM	2.5 ± 1.3	7.6 ± 2.2*	8.3 ± 1.9#	11.0 ± 1.8*; #
rVLM	2.5 ± 0.6	9.7 ± 2.0*	8.6 ± 2.8#	10.9 ± 3.0
RTN/pFRG	4.2 ± 2.9	5.3 ± 1.8	5.2 ± 1.8	3.8 ± 1.6
RPa	2.0 ± 1.4	6.3 ± 1.6*	5.4 ± 1.6#	4.8 ± 1.0
ROb	3.0 ± 0.8	7.6 ± 2.5*	5.5 ± 1.1	9.6 ± 3.6*
RMg	2.0 ± 1.3	4.0 ±1.7	3.4 ± 1.7	4.4 ± 1.8

Mean ± SD. VLM, ventrolateral reticular nucleus of the medulla; RTN/pFRG, retrotrapezoid nucleus/parafacial respiratory group; RPa, raphe palidus nucleus; RMg, raphe magnus nucleus; ROb, raphe obscurus nucleus; PP: Parapyramidal area; cNTS, commissural part of the nucleus tractus solitary; mNTS, medial part of the nucleus tractus solitary; vlNTS, ventrolateral part of the nucleus tractus solitary. Experiments were analysed using 2-way ANOVA completed by Tukey's post hoc test for multiple comparisons. * $p<0.05$ Normoxia *vs* Hypoxia (same genotype); # $p<0.05$ WT *vs* *Kcnk3*$^{\Delta 94ex1/\Delta 94ex1}$ rats.

Figure Legends

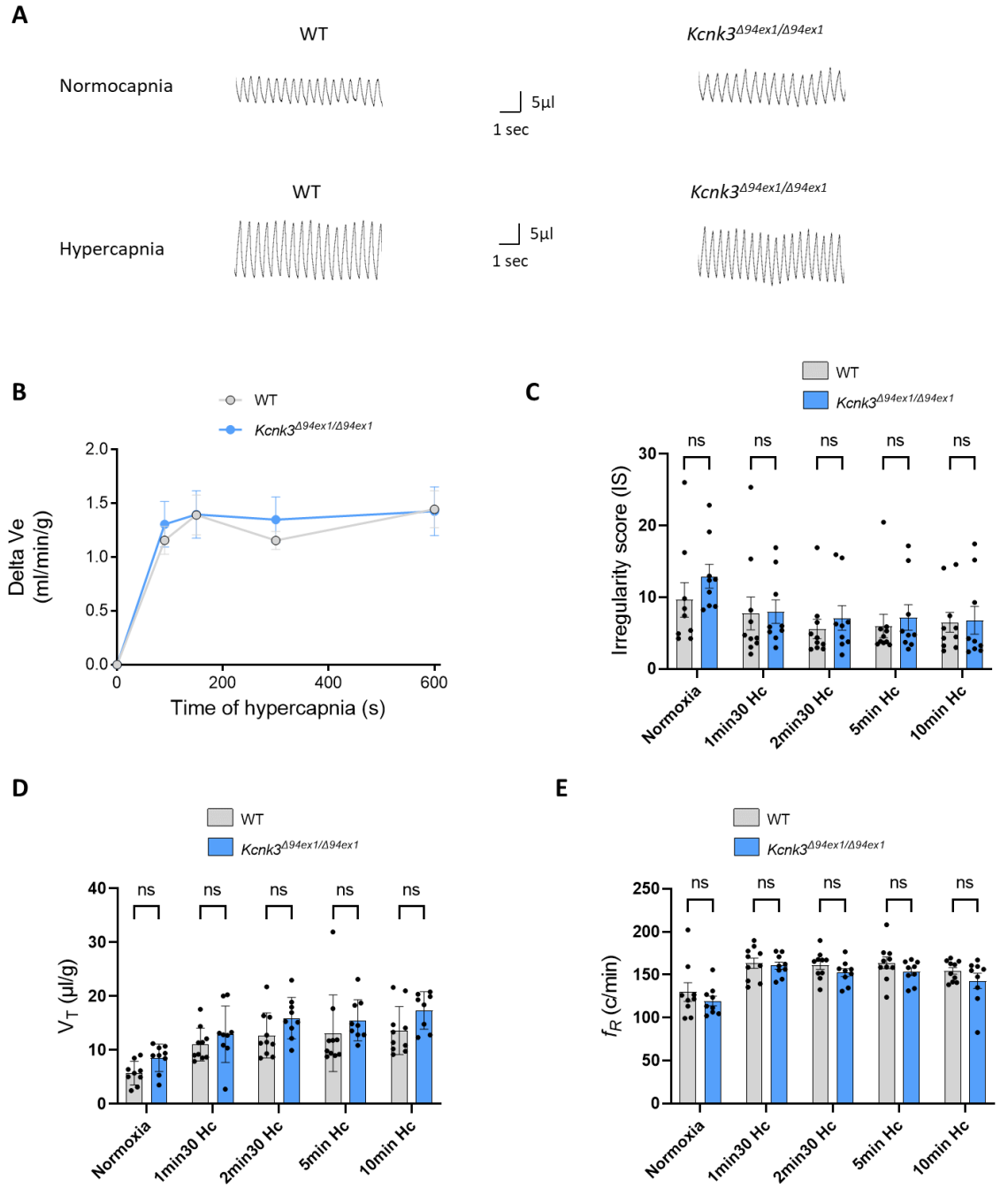

Figure 1

Figure 1: KCNK3/TASK-1 dysfunction did not modify the central chemoreflex. (A) Plethysmographic traces from the same WT and *Kcnk3*$^{\Delta 94ex1/\Delta 94ex1}$ rats when breathing air (normocapnia) or hypercapnic (Hc) gas mixture at 10 min. **(B)** Evolution of the delta of Ve as a function of the time of exposure to hypercapnia in WT and *Kcnk3*$^{\Delta 94ex1/\Delta 94ex1}$ rats. **(C-E)** Histograms showing irregularity score **(C)**, V_T **(D),** and f_R **(E)** change in WT (grey columns) and *Kcnk3*$^{\Delta 94ex1/\Delta 94ex1}$ (blue columns) rats. ns: not

647 significant. n= 10 for WT and n= 9 for *Kcnk3*$^{\Delta 94ex1/\Delta 94ex1}$. The black line and blue line correspond to basal
648 values for WT and *Kcnk3*$^{\Delta 94ex1/\Delta 94ex1}$, respectively. Experiments were analysed with 2-way ANOVA
649 completed by Tukey post hoc test for multiple comparisons. ns indicates nonsignificant, *p<0.05,
650 **p<0.01.

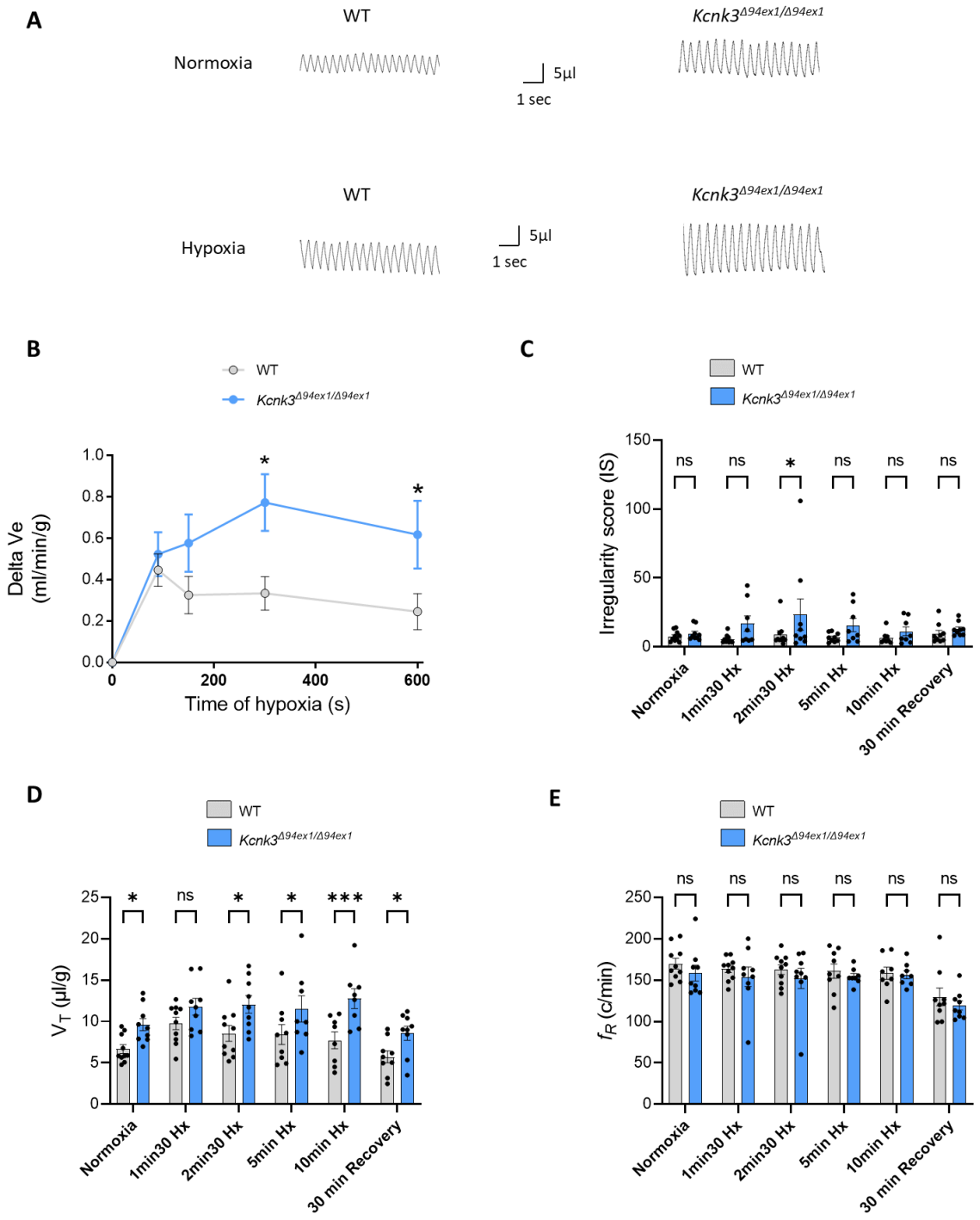

Figure 2

651

Figure 2: KCNK3/TASK-1 dysfunction alters the peripheral chemoreflex. (A) Plethysmographic traces from the same WT and *Kcnk3*$^{\Delta 94ex1/\Delta 94ex1}$ rats when breathing air (normoxia) or hypoxic (Hx) gas mixture at 5 min. **(B)** Evolution of the delta of Ve as a function of the time of exposure to hypoxia in WT and *Kcnk3*$^{\Delta 94ex1/\Delta 94ex1}$ rats. **(C-E)** Histograms showing irregularity score **(C)**, V_T **(D),** and f_R **(E)** change in WT (grey columns) and *Kcnk3*$^{\Delta 94ex1/\Delta 94ex1}$ (bleu columns) rats. n= 10 for WT and n= 9 for *Kcnk3*$^{\Delta 94ex1/\Delta 94ex1}$. The black line and blue line correspond to basal values for WT and *Kcnk3*$^{\Delta 94ex1/\Delta 94ex1}$, respectively. Experiments were analysed with 2-way ANOVA completed by Tukey post hoc test for multiple comparisons. ns indicates nonsignificant, *p<0.05, **p<0.01.

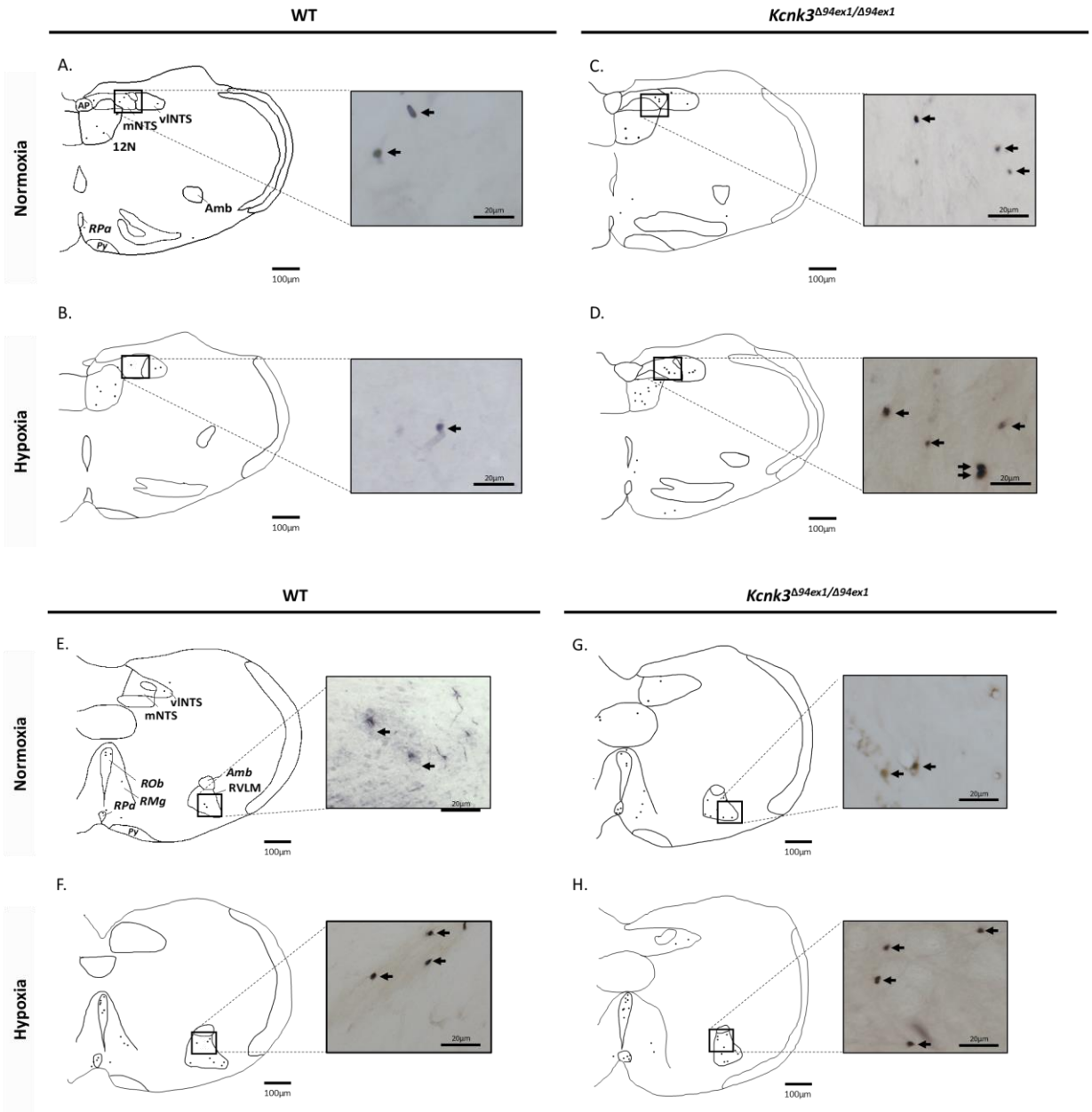

Figure 3: Representative labelling showing c-FOS expression in WT and *Kcnk3*-deficient rats exposed to normoxic or hypoxic conditions.

Drawings from several representative sections showing the distribution of the c-FOS positive cells (black dots) in the respiratory-related structure in WT (A, B, E, F) and *Kcnk3*$^{\Delta 94ex1/\Delta 94ex1}$ (C, D, G, H) rats exposed to normoxia (A, E, C, G) or Hypoxia (B, F, D, H). Scale bar = 100 µm. Abbreviations:12N, hypoglossal nucleus; Amb, ambiguous nucleus; AP: Area postrema; Py, pyramidal tract; RMg, raphe magnus nucleus; RPa, raphe pallidus nucleus; ROb, raphe obscurus nucleus; cNTS, commissural part of the nucleus of the solitary tract; mNTS, median part of the nucleus of the solitary tract; vlNTS, ventrolateral part of the nucleus of the solitary tract. n= 4 for WT rats in normoxia, n= 9 for WT rats in hypoxia, n= 10 for *Kcnk3*$^{\Delta 94ex1/\Delta 94ex1}$rats in normoxia and n= 8 for *Kcnk3*$^{\Delta 94ex1/\Delta 94ex1}$rats in hypoxia.